RNA & DISEASE 2014; 1: e441. doi: 10.14800/rd.441; © 2014 by Christopher Veigaard, *et al*.
http://www.smartscitech.com/index.php/rd

BRIEF REPORT

microRNA global expression analysis and genomic profiling of the camptothecin-resistant T-ALL derived cell line CPT-K5

Christopher Veigaard[1], Eigil Kjeldsen[2]

[1]*Cancercytogenetics Section, HemoDiagnostic Laboratory, Aarhus University Hospital, Tage-Hansens Gade 2, Ent. 4A, DK-8000 Aarhus C, Denmark*
[2]*Cancercytogenetics Section, HemoDiagnostic Laboratory, Aarhus University Hospital, Tage-Hansens Gade 2, Ent. 4A, DK-8000 Aarhus C, Denmark*

Correspondence: Eigil Kjeldsen
E-mail: Eigil.Kjeldsen@clin.au.dk
Received: April 21, 2014
Published: December 19, 2014

The clinical use of the camptothecin (CPT) derivatives, topotecan and irinotecan, has had a significant impact on cancer therapy. However, acquired clinical resistance to these drugs is common, which greatly hampers their clinical efficacy. MicroRNAs (miRNAs) is an exciting novel class of endogenous non-coding RNAs that negatively regulate gene expression of up to 50% of the protein-coding genes at the post-translational level. Abnormal expression of miRNAs is associated with pathogenesis of cancer and is also implicated in anticancer drug resistance phenotypes. We used global expression analysis to examine for differential miRNA expression between the camptothecin-resistant cell line CPT-K5 and its parental CPT-sensitive RPMI-8402. In the CPT-K5 cell line 18 miRNAs were deregulated. Fifteen of these were down-regulated and three were up-regulated. The miRNA-193a-3p, miR-130a-3p, and miR-29c-3p were the most down-regulated miRNAs at 205.9-fold, 33.9-fold and 5.5-fold, respectively, while the miRNA let-7i-5p was the most up-regulated at 3.9-fold. We used subtraction BAC-based array CGH analysis to examine for genomic copy number changes. Only for the three most down-regulated miRNAs a positive correlation was found with genomic loss of their chromosomal regions in which they are encoded. Potential functional targets of the differentially expressed miRNAs were examined by searching the miRBase and miRTarBase databases. Recurrent KEGG pathways that theoretically could be affected by the deregulated miRNAs are lysine degradation, cell cycle, PI3K-Akt-, ERbB- and p53- signaling pathways. We show that the intracellular levels of several miRNAs are significantly deregulated upon acquisition of CPT resistance in the T-ALL derived cell line CPT-K5, and that genomic copy number changes is not a major cause of deregulation. In addition, the most deregulated miRNAs in our study have previously been described to be involved in various types of chemotherapeutic resistance, including the chemotherapeutics CPT, gefitinib and cisplatin in other cancer and cell types. Our study adds to the current knowledge of the mechanisms of acquired CPT resistance. Specific miRNAs may prove to be future targets to reverse or inhibit development of CPT resistance thereby providing means for a more effective treatment.

Keywords: Camptothecin; drug resistance, leukemia cell lines; T-cell, CPT-K5; miRNA; microarray; aCGH

To cite this article: Christopher Veigaard, *et al*. microRNA global expression analysis and genomic profiling of the camptothecin-resistant T-ALL derived cell line CPT-K5. RNA Dis 2014; 1: e441. doi: 10.14800/rd.441.

Introduction

Camptothecin (CPT) specifically inhibits the nuclear enzyme DNA topoisomerase I (Top1) [1, 2]. Its effect is exerted by binding to the covalent complex formed by DNA and Top1 leading to persistent DNA breaks that are turned into devastating double stranded breaks (DSBs) upon collision with the replication or transcription machinery [3].

When these DSBs are unrepaired it confers apoptosis of the malignant cells and eventually eradication of the tumor [3].

The water-soluble CPT derivatives such as topotecan and irinotecan belong to a class of chemotherapeutic drugs that have been approved for treatment of various malignancies, including colorectal, ovarian, small cell lung cancers, leukemias and lymphomas [4]. However, their clinical efficacy is greatly hampered by development of resistance against CPT and its derivatives [5]. Reversing or inhibiting CPT resistance may provide means for a more effective treatment. Preclinical studies have shown that "classical" cellular alterations, such as drug-efflux, metabolism, Top1-down regulation, *TOP1* mutation and DNA damage response contribute to the CPT-resistance. However, recent lines of evidence have suggested new resistance mechanisms involving microRNA (miRNA) deregulation [6].

More than 2,500 human miRNAs have been identified. They belong to a class of non-coding RNA that is 20 to 25 nucleotides in length. The precise mechanisms of miRNA function have not been fully clarified yet. It is known, however, that each miRNA can regulate the expression of up to hundreds of target genes simultaneously, while a single gene can also be targeted by multiple miRNAs. The miRNAs control 30-50% of the protein-coding genes [7] and are therefore involved in a multitude of signaling pathways controlling normal cell differentiation, division, and apoptosis [8, 9]. There is strong evidence that dysregulated miRNAs can cause cancer and its progression [10]. However, it remains to be elucidated how they affect the response of cancer cells to chemotherapeutic treatment, in particular their involvement in acquisition of CPT resistance in leukemic cells. In one study it was shown that mRNA and miRNA expression profiles correlated with sensitivity to FdUMP[10], fluorouracil, floxuridine, topotecan, and irinotecan across a NCI-60 cell line screen [11]. In another study it was shown that 25 miRNAs were deregulated in intrinsic CPT resistance in gastric cancer derived cell lines [12].

To explore miRNA's role in acquired camptothecin resistance we took advantage of the camptothecin resistant cell line CPT-K5 and its parental RPMI-8402 and compared their global miRNA expression. The CPT-K5 cell line was previously developed by stepwise increasing exposure of the human T-ALL derived cell line RPMI-8402 to the CPT-derivative irinotecan [13]. Later we showed that the CPT-resistance correlated with a mutation at amino acid residue 533 (p.D533G, Asp->Gly) in the DNA binding domain of the Top1 enzyme [14]. The mutant enzyme acquired altered biochemical properties, especially as to how it interacts with DNA. The changed properties resulted in a higher efficiency for recognition of specific sequences and a higher stability of cleavable complexes contributing to the cellular CPT-resistance [15].

In the present study we show that 18 miRNAs are differently expressed between CPT-K5 and RPMI-8402 and that two miRNA's, miR-130a-3p and miRNA-193a-3p, were the most deregulated by a magnitude of 33.9- and 205.9-fold, respectively. In addition, we explored whether the deregulated miRNA expression correlated with changes in genomic copy numbers between the cell lines.

Materials & Methods

Cell cultures and purification of nucleic acids

The cell lines CPT-K5 and RPMI-8402 were cultured as described [15]. Five million cells in exponentially growth phase were used for RNA purifications with the miRNeasy Mini Kit (Qiagen Nordic, Solna, Sweden) according to manufacturer's protocol. DNA from three million cells was purified using the Gentra Puregene Blood Kit (Qiagen).

Microarray-based investigation of miRNA expression

Global miRNA expression profiles were obtained using miRCURY LNA™ microRNA Arrays (Exiqon, Vedbæk, Denmark). Two dual-color microarrays (version 208001V8.1) were used in a dye-swap setup with each sample (RNA from CPT-K5 and RPMI-8402) labelled with opposite fluorophores in the two hybridizations. Three micrograms of RNA was used for each labeling reaction and the matching labeling Kit from Exiqon was used according to protocol. Upon labeling the RNA was hybridized to the microarrays in an automated Tecan HS400 Pro hybridization station according to Exiqon's recommendations. The arrays were scanned at 532 and 635 nm in a GenePix 4000B scanner using the GenePix Pro 6.1 software (Molecular Devices, Sunnyvale, California, USA). The raw image files were analyzed in GenePix Pro 6.1 using a Gal-file annotated in compliance with miRBase release 11 [16]. Individual features were identified as irregular and the background subtraction was calculated using the "Morphologic opening" setting. Features with intensities below threshold (negative controls + 5SD) were excluded, and only features representing known human miRNAs where at least three of the four replicated spots had passed the above mentioned criteria were considered present and used in the subsequent analysis. The data from the two hybridizations were normalized using the global lowess algorithm in Acuity 4.0 (Molecular Devices). The normalized data from the dye-swap procedure were averaged to provide the final data. All miRNA names are reported according to the

Table 1. miRNA expression differences and copy number changes in CPT-K5 relative to RPMI-8402

microRNA name[a]	Pre-microRNA	Cytoband	Genomic position (bp)	Mean (log_2)	Fold change	Copy number change
Up-regulated						
1. hsa-let-7i-5p		12q14.1	61,283,733-61,283,816	1,95	3,9	NC
2 hsa-miR-7-5p[b]	2a. hsa-miR-7-5p-1	9q21.32	85,774,483-85,774,592	1,51	2,9	NC
	2b. hsa-miR-7-5p-2	15q26.1	86,956,060-86,956,169			NC
	2c. hsa-miR-7-5p-3	19p13.3	4,721,682-4,721,791			NC
3. hsa-miR-29a-3p		7q32.3	130,212,046-130,212,109	1,28	2,4	NC
Down-regulated						
4. hsa-miR-193a-3p		17q11.2	26,911,128-26,911,215	-7,69	-205,9	Loss
5. hsa-miR-130a-3p		11q12.1	57,162,547-57,165,335	-5,08	-33,9	Loss
6. hsa-miR-29c-3p		1q32.2	206,041,820-206,041,907	-2,46	-5,5	Loss
7. hsa-miR-146b-5p		10q24.32	104,186,259-104,186,331	-2,43	-5,4	NC
8. hsa-miR-21-5p		17q23.1	55,273,409-55,273,480	-2,39	-5,2	Loss
9. hsa-miR-26a-5p[b]	9a. hsa-miR-26a-5p-1	3p22.2	37,985,899-37,985,975	-2,19	-4,6	Gain
	9b. hsa-miR-26a-5p-2	12q24.1	56,504,659-56,504,742			NC
10. hsa-miR-103-3p[b]	10a. hsa-miR-103-3p-1	5q34	168,560,896-168,560,973	-1,92	-3,8	NC
	10b. hsa-miR-103-3p-2	20p13	3,917,494-3,917,571			NC
11. hsa-miR-106b-5p		7q22.1	99,529,552-99,529,633	-1,63	-3,1	Gain
12. hsa-miR-222-3p		Xp11.3	45,491,365-45,491,474	-1,61	-3,1	Loss
13. hsa-miR-15b-5p		3q25.33	161,605,070-161,605,167	-1,59	-3,0	Loss
14. hsa-miR-18a-5p		13q31.3	90,801,006-90,801,076	-1,45	-2,7	Gain
15. hsa-miR-18b		Xq26.2	133,131,737-133,131,807	-1,38	-2,6	Loss
16. hsa-miR-30c-5p[b]	16a. hsa-miR-30c-5p-1	1p34.2	40,995,543-40,995,631	-1,22		Loss
	16b. hsa-miR-30c-5p-2	6q13	72,143,384-72,143,455		-2,3	NC
17. hsa-miR-142-3p		17q22	53,763,592-53,763,678	-1,16	-2,2	Loss
18. hsa-miR-183-5p		7q32.2	129,201,981-129,202,090	-1,13	-2,2	NC

[a] microRNAs are named according to miRBase 20. [b] microRNAs with more than one genomic location although it is only possible to measure the overall expression of the respective microRNAs. NC refers to no copy number change. bp refers base pair.

nomenclature used in miRBase 20. Exempted from this rule is data referenced from earlier publications, where miRNA names are reported according to the nomenclature used in the original publications.

qPCR analysis of miRNA expression

Specific miRNA expression were investigated by qPCR using TaqMan^R MicroRNA Assays (Life Technologies Europe, Nærum, Denmark) according to protocol. The Mx3000P RQ-PCR System (Agilent Technologies, Santa Clara, CA, USA) was used for the PCR reactions and output data were analyzed by the ΔC_t relative quantification model using RNU6B and RNU48 (Life Technologies Europe) as reference genes for normalization.

Array-based comparative genomic hybridization analysis

Array-based comparative genomic hybridization (aCGH) analysis was done using the CytoChip BAC-array platform (BlueGnome, Cambridge, UK) as previously described [17]. CPT-K5 DNA was labeled with Cy3 and RPMI-8402 DNA with Cy5. The GenePix 4000B laser scanner (Molecular Devices) together with GenePix Pro 6.1 software (Molecular Devices) was used to scan he microarray. The CytoChip algorithm analysis tool in the BlueFuse 3.5 software (BlueGnome) defined regions of gain or loss. Reference genome was NCBI build 36.1 (hg18). Bioinformatics analysis was performed by querying the UCSC database (http://genome.ucsc.edu).

Results

Comparison of miRNA profiles between CPT-K5 and RPMI-8402

We examined whether differential miRNA expression between the camptothecin-resistant CPT-K5 and its parental camptothecin-sensitive RPMI-8402 cell line could be detected using a miRNA microarray platform from Exiqon. This microarray contains 5924 probes representing 429 miRNAs, and 94 miRNAs were expressed above threshold (Supplemental Table 1). Eight-teen miRNAs emerged as differently expressed by more than a 2-fold change in the CPT-K5 cell line compared with RPMI-8402 (Table 1). Specifically, fifteen miRNAs were down-regulated and three were up-regulated in CPT-K5. The miRNA-193a-3p and miR-130a-3p, were the most down-regulated miRNAs at 205, 9-fold and 33.9-fold, respectively, while the miRNA let-7i-5p was the most up-regulated at 3.9-fold.

To validate the microarray data, four differently expressed genes were randomly chosen for validation by Taqmann MicroRNA assays. The selected miRNAs were up-regulated (miR-7-5p), down-regulated (miR-18a-5p and miR-130a-3p) or showed no change in expression (miR-223-3p) (Figure 1A). The expression levels of the miRNAs from real time PCR were consistent with results from miRNA array

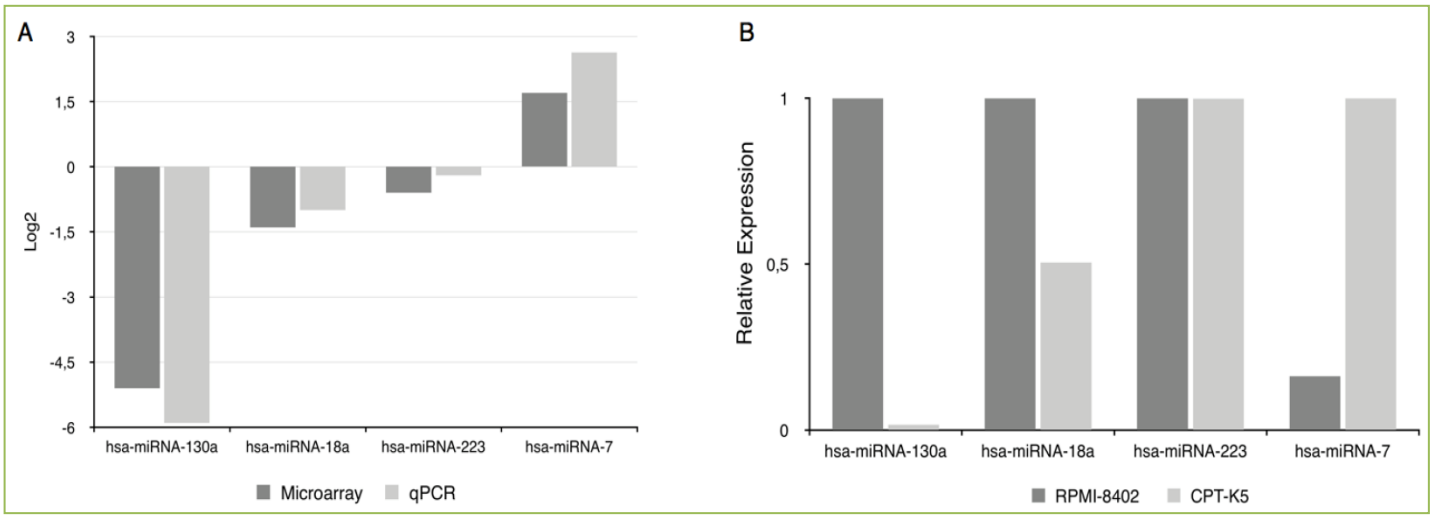

Figure 1. Analysis of miRNA expression. Panel A. Comparison of microarray-based and qPCR-based measurements of selected miRNAs. Log_2 values for expression of miR-130a-3p, miR-18a-5p, miR-223-3p, and miR-7-5p in CPT-K5 relative to RPMI-8402 are shown. Dark and light grey bars represent data from microarray and qPCR measurements, respectively. Panel B. Fold difference in expression of indicated miRNAs measured by qPCR. Means from triplicate experiments are indicated. Dark and light grey bars represent data from RPMI-8402 and CPT-K5, respectively.

analysis. A comparison of expression levels between CPT-K5 and RPMI-8402 was done by real time PCR confirming the observed differences in expression of the miRNAs, miR-7-5p, miR-18a-5p and miR-130-3p, and no change of miR-223-3p as also determined by the microarray analysis (Figure 1B).

Comparison of differently expressed miRNAs and copy number changes of CPT-K5 and RPMI-8402

To evaluate a possible correlation between differently expressed miRNAs and genomic copy number changes we performed subtractive whole genome profiling to analyze for copy number changes between CPT-K5 and RPMI-8402 using a BAC-based aCGH microarray. Sixty-one genomic regions emerged as regions of copy number changes between CPT-K5 and RPMI-8402 (Figure 2A, and Supplemental Table 2). Specifically, 32 regions were gained while 29 regions showed copy number losses. We examined the copy number changes relative to the genomic positions of the differently expressed miRNAs (Table 1, Figure 2B). In the group of up-regulated miRNAs we observed for all miRNAs no copy number changes between CPT-K5 and RPMI-8402. In the group of down-regulated miRNAs nine (9/18, 50%) were located in regions of copy number losses, three (3/18, 17%) were located in regions of copy number gains and six (6/18, 33%) were located in regions of no copy number changes.

For the three most highly down-regulated miRNAs (miR-193a-3p, hmiR130a-3p, and miR-29c-3p) there were a correlation between their location in genomic regions with copy number losses while for the rest of the miRNAs there were no correlation with their differences in expression levels and copy number changes.

miRNA targets of the changed miRNAs

To identify potential functional miR-targets of the deregulated miRNAs the DIANA-miRPath (http://diana.imis.athena-innovation.gr) were searched (Table 2). Recurrent KEGG pathways that theoretically might be affected by the deregulated miRNAs are lysine degradation, cell cycle, PI3K-Akt-, ERbB- and p53- signaling pathways.

Discussion

In the present study we showed that 18 miRNAs are deregulated during acquisition of resistance to the camptothecin derivative irinotecan in the CPT-K5 cell line. By comparing the miRNA differences with genomic copy number changes between the two cell lines the expression of the most down-regulated miRNAs (≥ 5.5-fold decrease) correlated with identified genomic losses. The most deregulated miRNAs were miR-193a-3p, miR-130a-3p, and miR-29c-3p exhibiting a 205.9-, 33.9-, and 5.5-fold decrease in expression, respectively. For the remaining 15 deregulated miRNAs no correlation between their relative expression level and genomic copy number status was found. These findings indicate that high expression changes are more likely associated with copy number changes compared to moderate or minor expression changes. This notion is supported by the findings that massive up-regulation of MYC expression is associated with high-level amplification of the MYC oncogene [18], and that massive down-regulation is associated with gene deletions [19]. When moderate or minor expression changes are observed other factors than copy number changes may influence their expression level [10, 20]. The miRNA expression is mainly regulated in a tissue-specific and disease state-specific fashion by different transcription factors while some miRNAs are regulated by

Table 2. KEGG analysis

MicroRNA (version 20)	KEGG pathway(s)[a]
hsa-let-7i-5p	Lysine degradation, Circadian entrainment
hsa-miR-7-5p	Glioma, Insulin signaling pathway, Melanoma, Non-small cell lung cancer, Regulation of actin cytoskeleton, ErbB signaling pathway, Neurotrophin signaling pathway, HIF-1 signaling pathway, GnRH signaling pathway, Endometrial cancer, Prostate cancer
hsa-miR-29a-3p	Focal adhesion, Small cell lung cancer, ECM-receptor interaction, PI3K-Akt signaling pathway
hsa-miR-183-5p	N.D.
hsa-miR-142-3p	N.D.
hsa-miR-30c-5p	Base excision repair
hsa-miR-18b-5p	Endocrine and other factor-regulated calcium reabsorption
hsa-miR-18a-5p	Cell cycle, Chronic myeloid leukemia, Rheumatoid arthritis, Colorectal cancer, Hepatitis B, Pathways in cancer
hsa-miR-15b-5p	Small cell lung cancer, Legionellosis, Pathways in cancer, Prostate cancer, Epstein-Barr virus infection, Protein processing in endoplasmic reticulum, Toxoplasmosis, Hepatitis B, Cell cycle
hsa-miR-222-3p	PI3K-Akt signaling pathway, Mucin type O-Glycan biosynthesis, p53 signaling pathway, Measles, Pathways in cancer
hsa-miR-106b-5p	Prion diseases, Bladder cancer, Influenza A, Cell cycle, Pancreatic cancer, Prostate cancer, Glioma
hsa-miR-103a-3p	Cell cycle, p53 signaling pathway, Small cell lung cancer, Non-small cell lung cancer, Melanoma, Chronic myeloid leukemia, Steroid biosynthesis, Pancreatic cancer, Glioma, Measles
hsa-miR-26a-5p	Cell cycle, TGF-beta signaling pathway, Hepatitis B, p53 signaling pathway, PI3K-Akt signaling pathway, Colorectal cancer, Small cell lung cancer, Prostate cancer
hsa-miR-21-5p	Pathways in cancer, Colorectal cancer, Hepatitis B, Pancreatic cancer, Bladder cancer, p53 signaling pathway, Small cell lung cancer, Endometrial cancer, Chronic myeloid leukemia, Prostate cancer, HIF-1 signaling pathway, ErbB signaling pathway, MAPK signaling pathway, Lysine degradation
hsa-miR-146b-5p	NF-kappa B signaling pathway, Toll-like receptor signaling pathway, Neurotrophin signaling pathway, Hepatitis B, Pertussis, Leishmaniasis, Chagas disease (American trypanosomiasis), Epstein-Barr virus infection, Hepatitis C, Measles
hsa-miR-29c-3p	ECM-receptor interaction, Protein digestion and absorption, Focal adhesion, Amoebiasis, PI3K-Akt signaling pathway, Small cell lung cancer
hsa-miR-130a-3p	Prion diseases, Cell cycle, Viral carcinogenesis
hsa-miR-193a-3p	N.D.

[a] According to DIANA-miRPath (REF) - http://diana.imis.athena-innovation.gr/DianaTools/index.php?r=mirpath/index. Search based on interactions derived from the TarBase with FDR Correction and Conservative Stats applied. P-value threshold set at 0.01. N.D. No data.

tumor suppressor or oncogene pathways such as TP53, MYC and RAS [21]. Deregulated miRNA expression can also result from changes in epigenetic regulation, such as methylation status of miRNA genes [22] or may result from mutations in miRNA genes [23].

Altered intracellular levels of miRNAs interfere with the chemoresponses in a variety of cancer cells [11, 12, 24-26]. In a study utilizing the NCI-60 cell line panel it was shown that mRNA and miRNA expression profiles correlated with sensitivity to FdUMP[10], fluorouracil, floxuridine, topotecan, and irinotecan [11]. In a study of the CPT-resistant colon cancer cell line SW1116/HCPT, seventy-seven miRNAs were differentially expressed compared to its parental SW1116 (30 miRNAs were down-regulated and 47 were up-regulated) [25]. Among these miRNAs the miR-548d was the highest up-regulated (124.55-fold) while miR-641 was the most down-regulated (60.20-fold). The authors also performed differential gene expression showing that PPAR expression was the highest down-regulated (404.1-fold), and that it is one of the target genes of miR-506, which was over-expressed. PPAR has been shown to regulate some MDR proteins, which uses ATP to extrude chemotherapeutic agents from the cells [27]. Intrinsic drug resistance to hydroxycamptothecin was studied in six gastric cancer cell lines and it was shown that 25 miRNAs were deregulated in the resistant cells, including up-regulated miR-196a, miR-338, miR-126, miR-98, let-7g, and

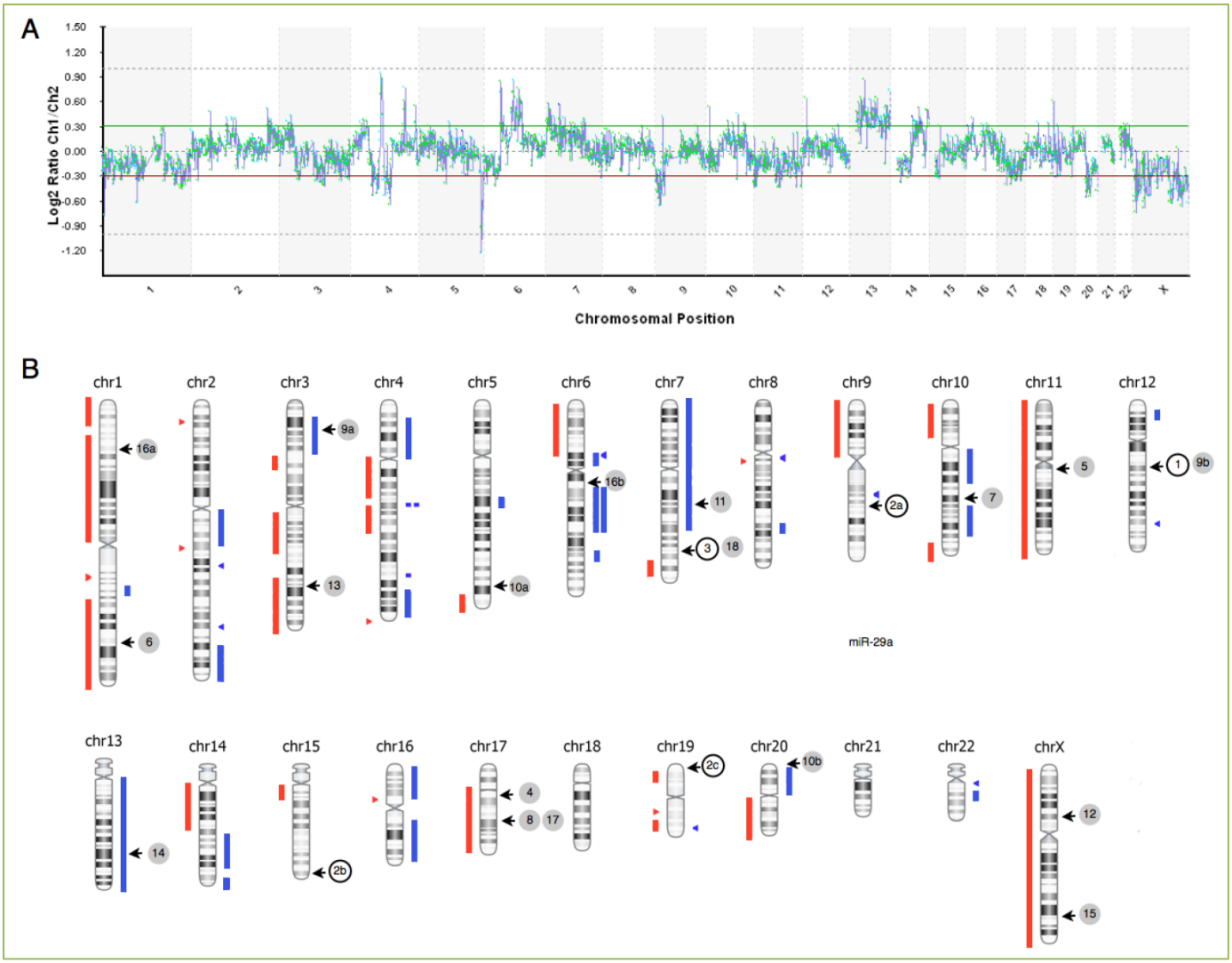

Figure 2. Analysis of genomic copy number changes. Panel A. CPT-K5 genome chart view of BAC-based aCGH profile where RPMI-8402 is used as reference genome. Chromosomal position is specified on the x-axis and $\log^2$ ratio on the y-axis. Panel B. Chromosome view of called regions. Blue bars next to the chromosomal ideograms indicate regions of gain and red bars indicate regions of losses. Chromosomal positions of miRNAs that are differently expressed in CPT-K5 relative to RPMI-8402 are indicated by open (up-regulated) or closed (down-regulated) circles where the numbers in the circles refer to the miRNAs listed in Table 1.

down-regulated miR-200 family, miR-31, and miR-7 [12]. In our study we found that let-7i-5p and miR-7-5p were the two most up-regulated and that miR-193a-3p, miR-130a-3p, and miR-29c-3p were the three most down-regulated miRNAs. Comparing our differential expression miRNA results with the previous studies on CPT resistance in various cell lines and cell types it is only the miR-7-5p that is a recurrent miRNA involved in CPT resistance. We found that miR-7-5p was up-regulated while Wu *et al.* found it to be down-regulated [12].

The disparate results between the different studies may be explained by variations in the molecular pathways in the different cancer cells. It should be noted that miRNAs execute their biological function via repression of many different protein-coding genes involved in a multitude of signaling pathways. Another reason could be the effect of local tumor microenvironment, which is well known to be modulated via a variety of signaling networks [28].

The most deregulated miRNA in our study was the 205.9-fold down- regulation of miR-193a-3p in the acquired CPT resistance of the CPT-K5 cell line. Its aberrant expression has been reported in all the types of cancer examined, including colorectal cancer [29], non-small cell lung cancer (NSCLC) [30], myeloid leukemia [31] and Wilms' tumor blastema [32]. The transcription factors XB130 [33], and p63 [34] have been implicated in the regulation of miR-193a expression as well as the DNA methylation state of its promotor region [35]. A tumor-suppressor role of miR-193a-3p has been reported in NSCLC [30] and epithelial ovarian cancer cells [36]. Conversely, miR-193a-3p can also

promote both *in vivo* growth and chemo-resistance of hepatocellular carcinoma [35] and bladder cancer cells [37]. The bladder cancer cell line 5637 is chemosensitive when the promotor of miR-193a is hypermethylated while the chemoresistant bladder cancer cell line is drug resistant because of a hypomethylated promotor [38]. Four direct target genes of miR-193a-3p were identified (PLAU, HIC2, SRSF2 and LOXL4) conveying bladder cancer multi-chemoresistance against various chemotherapeutic drugs, including etoposide, carboplatin, cisplatin, 5-fluorocil, and doxorubicin. Resistance against CPT has not prior to our study been associated with deregulated miR-193a-3p expression.

The second-most down-regulated miRNA in our study was miRNA-130a-3p exhibiting a 33.9-fold down-regulation. miR-130a plays a crucial role in tumor biology with different functions in various cancers acting as both an oncogene (NSCLC, cervical cancer and colorectal cancer) and as a tumor suppressor gene (glioblastoma, prostate cancer and leukemia) [39]. The reasons for the apparently contradictory roles of miR-130a are not clear. Recently, it was shown that miR-130a under-expression leads to gefitinib resistance in NSCLC whereas overexpression increases sensitivity to gefitinib [40]. The MET gene was shown to be a direct target of miR-130a and that MET amplification leads to gefitinib resistance by activating the ERBB3 signaling pathway. In ovarian cancer it was shown that under-expression conferred cisplatin-resistance by targeting X-linked inhibitor of apoptosis [41]. In hepatocellular carcinoma (HCC) miR-130a increases drug resistance by regulating RUNX3 and wnt signaling in cisplatin treated HCC [39]. Taken together these findings indicate that a common drug resistance mechanism may be ascribed to miR-130a.

We observed that the miR-29c-3p was down-regulated by 5.5-fold. miR-29c has been identified as a tumor suppressor in several human cancers [42]. Low expression of miR-29c was recently shown to be positively associated with therapeutic resistance in 159 nasopharyngeal carcinoma cases against ionizing radiation and cisplatin [43]. The authors also showed that expression of the anti-apoptotic factors, MCL-1 and BCL-2 in NPC tissues and cell lines were repressed by miR-29c.

Conclusions

Our present study demonstrates that the intracellular levels of certain miRNAs are significantly deregulated upon acquisition of camptothecin resistance. We show a positive correlation of genomic losses and miRNAs down-regulated by ≥5.5-fold. Interestingly, all major deregulated miRNAs described in our study have previously been described in other cancer and cell types to be involved in various types of chemotherapeutic resistance, including CPT, gefitinib and cisplatin. Our study adds to a better understanding onto which miRNAs that might have a role in resistance to CPT and its derivatives. Resistance to CPT limits its clinical efficacy and by knowing which miRNAs that are involved in the resistance mechanism future experiments with direct miRNA targets may be designed to examine whether it'll be possible to reversing such resistance or to avoid its development.

Acknowledgements

The Danish Cancer Society supported the study.

Conflict of interests

The authors have no conflicting interests to declare.

References

1. Hsiang YH, Hertzberg R, Hecht S, Liu LF. Camptothecin induces protein-linked DNA breaks via mammalian DNA topoisomerase I. J Biol Chem 1985; 260:14873-14878.
2. Kjeldsen E, Mollerup S, Thomsen B, Bonven BJ, Bolund L, Westergaard O. Sequence-dependent effect of camptothecin on human topoisomerase I DNA cleavage. J Mol Biol 1988; 202:333-342.
3. Pommier Y. Topoisomerase I inhibitors: camptothecins and beyond. Nature reviews Cancer 2006; 6:789-802.
4. Zunino F, Pratesi G. Camptothecins in clinical development. Expert opinion on investigational drugs 2004; 13:269-284.
5. Beretta GL, Gatti L, Perego P, Zaffaroni N. Camptothecin resistance in cancer: insights into the molecular mechanisms of a DNA-damaging drug. Current medicinal chemistry 2013; 20:1541-1565.
6. Xing Z, Li D, Yang L, Xi Y, Su X. MicroRNAs and anticancer drugs. Acta biochimica et biophysica Sinica 2014; 46:233-239.
7. Miranda KC, Huynh T, Tay Y, Ang YS, Tam WL, Thomson AM, *et al*. A pattern-based method for the identification of MicroRNA binding sites and their corresponding heteroduplexes. Cell 2006; 126:1203-1217.
8. Chen CZ, Li L, Lodish HF, Bartel DP. MicroRNAs modulate hematopoietic lineage differentiation. Science 2004; 303:83-86.
9. Hwang HW, Mendell JT. MicroRNAs in cell proliferation, cell death, and tumorigenesis. Br J Cancer 2006; 94:776-780.
10. Farazi TA, Spitzer JI, Morozov P, Tuschl T. miRNAs in human cancer. J Pathol 2011; 223:102-115.
11. Gmeiner WH, Reinhold WC, Pommier Y. Genome-wide mRNA and microRNA profiling of the NCI 60 cell-line screen and comparison of FdUMP[10] with fluorouracil, floxuridine, and topoisomerase 1 poisons. Molecular cancer therapeutics 2010; 9:3105-3114.
12. Wu XM, Shao XQ, Meng XX, Zhang XN, Zhu L, Liu SX, *et al*. Genome-wide analysis of microRNA and mRNA expression

signatures in hydroxycamptothecin-resistant gastric cancer cells. Acta pharmacologica Sinica 2011; 32:259-269.

13. Andoh T, Ishii K, Suzuki Y, Ikegami Y, Kusunoki Y, Takemoto Y, *et al*. Characterization of a mammalian mutant with a camptothecin-resistant DNA topoisomerase I. Proc Natl Acad Sci U S A 1987; 84:5565-5569.
14. Tamura H, Kohchi C, Yamada R, Ikeda T, Koiwai O, Patterson E, *et al*. Molecular cloning of a cDNA of a camptothecin-resistant human DNA topoisomerase I and identification of mutation sites. Nucleic acids research 1991; 19:69-75.
15. Kjeldsen E, Bonven BJ, Andoh T, Ishii K, Okada K, Bolund L, *0*. Characterization of a camptothecin-resistant human DNA topoisomerase I. J Biol Chem 1988; 263:3912-3916.
16. Griffiths-Jones S, Saini HK, van Dongen S, Enright AJ. miRBase: tools for microRNA genomics. Nucleic acids research 2008; 36:D154-158.
17. Veigaard C, Norgaard JM, Kjeldsen E. Genomic profiling in high hyperdiploid acute myeloid leukemia: a retrospective study of 19 cases. Cancer genetics 2011; 204:516-521.
18. Little CD, Nau MM, Carney DN, Gazdar AF, Minna JD. Amplification and expression of the c-myc oncogene in human lung cancer cell lines. Nature 1983; 306:194-196.
19. Li J, Liu Y, Liu M, Han JD. Functional dissection of regulatory models using gene expression data of deletion mutants. PLoS genetics 2013; 9:e1003757.
20. Veigaard C, Kjeldsen E. Exploring the genome-wide relation between copy number status and microRNA expression. Genomics 2014.
21. Krol J, Loedige I, Filipowicz W. The widespread regulation of microRNA biogenesis, function and decay. Nature reviews Genetics 2010; 11:597-610.
22. Han L, Witmer PD, Casey E, Valle D, Sukumar S. DNA methylation regulates MicroRNA expression. Cancer biology & therapy 2007; 6:1284-1288.
23. Ryan BM, Robles AI, Harris CC. Genetic variation in microRNA networks: the implications for cancer research. Nature reviews Cancer 2010; 10:389-402.
24. Robertson NM, Yigit MV. The role of microRNA in resistance to breast cancer therapy. Wiley interdisciplinary reviews RNA 2014; 5:823-833.
25. Tong JL, Zhang CP, Nie F, Xu XT, Zhu MM, Xiao SD, *et al*. MicroRNA 506 regulates expression of PPAR alpha in hydroxycamptothecin-resistant human colon cancer cells. FEBS Lett 2011; 585:3560-3568.
26. Gougelet A, Pissaloux D, Besse A, Perez J, Duc A, Dutour A, *et al*. Micro-RNA profiles in osteosarcoma as a predictive tool for ifosfamide response. Int J Cancer 2011; 129:680-690.
27. Fanciulli M, Valentini A, Bruno T, Citro G, Zupi G, Floridi A. Effect of the antitumor drug lonidamine on glucose metabolism of adriamycin-sensitive and -resistant human breast cancer cells. Oncol Res 1996; 8:111-120.
28. Bronisz A, Godlewski J, Wallace JA, Merchant AS, Nowicki MO, Mathsyaraja H, *et al*. Reprogramming of the tumour microenvironment by stromal PTEN-regulated miR-320. Nature cell biology 2012; 14:159-167.
29. Yong FL, Law CW, Wang CW. Potentiality of a triple microRNA classifier: miR-193a-3p, miR-23a and miR-338-5p for early detection of colorectal cancer. BMC cancer 2013; 13:280.
30. Heller G, Weinzierl M, Noll C, Babinsky V, Ziegler B, Altenberger C, *et al*. Genome-wide miRNA expression profiling identifies miR-9-3 and miR-193a as targets for DNA methylation in non-small cell lung cancers. Clin Cancer Res 2012; 18:1619-1629.
31. Gao XN, Lin J, Li YH, Gao L, Wang XR, Wang W, *et al*. MicroRNA-193a represses c-kit expression and functions as a methylation-silenced tumor suppressor in acute myeloid leukemia. Oncogene 2011; 30:3416-3428.
32. Watson JA, Bryan K, Williams R, Popov S, Vujanic G, Coulomb A, *et al*. miRNA profiles as a predictor of chemoresponsiveness in Wilms' tumor blastema. PloS one 2013; 8:e53417.
33. Takeshita H, Shiozaki A, Bai XH, Iitaka D, Kim H, Yang BB, *et al*. XB130, a new adaptor protein, regulates expression of tumor suppressive microRNAs in cancer cells. PloS one 2013; 8:e59057.
34. Ory B, Ramsey MR, Wilson C, Vadysirisack DD, Forster N, Rocco JW, *et al*. A microRNA-dependent program controls p53-independent survival and chemosensitivity in human and murine squamous cell carcinoma. J Clin Invest 2011; 121:809-820.
35. Ma K, He Y, Zhang H, Fei Q, Niu D, Wang D, *et al*. DNA methylation-regulated miR-193a-3p dictates resistance of hepatocellular carcinoma to 5-fluorouracil via repression of SRSF2 expression. J Biol Chem 2012; 287:5639-5649.
36. Nakano H, Yamada Y, Miyazawa T, Yoshida T. Gain-of-function microRNA screens identify miR-193a regulating proliferation and apoptosis in epithelial ovarian cancer cells. Int J Oncol 2013; 42:1875-1882.
37. Lv L, Deng H, Li Y, Zhang C, Liu X, Liu Q, *et al*. The DNA methylation-regulated miR-193a-3p dictates the multi-chemoresistance of bladder cancer via repression of SRSF2/PLAU/HIC2 expression. Cell death & disease 2014; 5:e1402.
38. Deng H, Lv L, Li Y, Zhang C, Meng F, Pu Y, *et al*. miR-193a-3p regulates the multi-drug resistance of bladder cancer by targeting the LOXL4 gene and the Oxidative Stress pathway. Molecular cancer 2014; 13:234.
39. Li B, Huang P, Qiu J, Liao Y, Hong J, Yuan Y. MicroRNA-130a is down-regulated in hepatocellular carcinoma and associates with poor prognosis. Med Oncol 2014; 31:230.
40. Zhou YM, Liu J, Sun W. MiR-130a overcomes gefitinib resistance by targeting met in non-small cell lung cancer cell lines. Asian Pacific journal of cancer prevention : APJCP 2014; 15:1391-1396.
41. Zhang X, Huang L, Zhao Y, Tan W. Downregulation of miR-130a contributes to cisplatin resistance in ovarian cancer cells by targeting X-linked inhibitor of apoptosis (XIAP) directly. Acta biochimica et biophysica Sinica 2013; 45:995-1001.
42. Wang Y, Zhang X, Li H, Yu J, Ren X. The role of miRNA-29 family in cancer. European journal of cell biology 2013; 92:123-128.
43. Zhang JX, Qian D, Wang FW, Liao DZ, Wei JH, Tong ZT, *et al*. MicroRNA-29c enhances the sensitivities of human nasopharyngeal carcinoma to cisplatin-based chemotherapy and radiotherapy. Cancer Lett 2013; 329:91-98.

Supplemental

Table1. Detailed summary of miRNA expression differences.

id	miRNA	Mean log2 value (CPT-K5/RPMI-8402)
17748	hsa-let-7a	-0.956
17749	hsa-let-7b	-0.031
19004	hsa-let-7c	-0.1105
17751	hsa-let-7e	0.202
19580	hsa-let-7i	1.947
10919	hsa-miR-103	-1.9245
17605	hsa-miR-106a/17	-0.564
19582	hsa-miR-106b	-1.6295
10923	hsa-miR-107	-0.199
10928	hsa-miR-125a-5p	0.1015
10934	hsa-miR-129-5p	-0.1535
10935	hsa-miR-130a	-5.0825
10936	hsa-miR-130b	-0.303
10947	hsa-miR-142-3p	-1.157
19015	hsa-miR-142-5p	-0.868
10306	hsa-miR-146b-5p	-2.4285
10964	hsa-miR-155	-0.0625
17280	hsa-miR-15b	-1.591
10967	hsa-miR-16	-0.9935
10977	hsa-miR-183	-1.1295
10978	hsa-miR-184	-0.03
5560	hsa-miR-185	0.0545
10983	hsa-miR-18a	-1.448
13141	hsa-miR-18b	-1.3845
10985	hsa-miR-191	-0.252
10986	hsa-miR-193a-3p	-7.6855
10993	hsa-miR-198	0.0755
10997	hsa-miR-19a	-0.608
11008	hsa-miR-20a	-0.318
10999	hsa-miR-20a	-0.098
5740	hsa-miR-21	-2.389
13511	hsa-miR-210	-0.0595
11014	hsa-miR-214	-0.0255
11023	hsa-miR-222	-1.6125
11024	hsa-miR-223	-0.6375
11026	hsa-miR-23a	-0.3005
11027	hsa-miR-23b	-0.656
11030	hsa-miR-26a	-2.1905
11039	hsa-miR-29a	1.278
11041	hsa-miR-29c	-2.458
17565	hsa-miR-30b	-0.457
17502	hsa-miR-30c	-1.2225
11054	hsa-miR-320	-0.4365
11069	hsa-miR-342-3p	0.0755
19018	hsa-miR-346	0.1315
14301	hsa-miR-361-5p	-0.3355
11082	hsa-miR-370	0.0455
11086	hsa-miR-373*	0.0785

11105	hsa-miR-378	0.9135
14306	hsa-miR-381	-0.1005
11097	hsa-miR-382	-0.0045
11106	hsa-miR-423-3p	0.093
13180	hsa-miR-483-3p	-0.196
11122	hsa-miR-490-3p	0.1275
11124	hsa-miR-492	-0.086
14287	hsa-miR-494	-0.088
11130	hsa-miR-498	-0.0925
11132	hsa-miR-500*/502-3p	0.14
11135	hsa-miR-503	-0.091
11142	hsa-miR-510	0.239
11145	hsa-miR-512-5p	0.157
11151	hsa-miR-516b	0.1785
11177	hsa-miR-518a-5p/527	0.227
13131	hsa-miR-518c*	0.0575
10586	hsa-miR-518d-5p/518f*/520c-5p/526a	0.231
13137	hsa-miR-518e*/519a*/519b-5p/519c-5p/522*/523*	0.245
13132	hsa-miR-519e*	0.163
10618	hsa-miR-524-5p	0.3235
11175	hsa-miR-525-5p	0.22
11176	hsa-miR-526b	0.2845
17272	hsa-miR-551a	0.061
17376	hsa-miR-557	0.0935
17551	hsa-miR-572	-0.3435
17295	hsa-miR-583	0.1945
17423	hsa-miR-584	0.1845
17498	hsa-miR-601	0.1065
17510	hsa-miR-602	-0.0995
17346	hsa-miR-612	0.114
17552	hsa-miR-617	0.057
17309	hsa-miR-623	-0.0775
17573	hsa-miR-625	0.1975
17471	hsa-miR-628-3p	0.0585
17566	hsa-miR-629*	0.1825
17327	hsa-miR-630	0.27
17550	hsa-miR-638	0.0275
17441	hsa-miR-648	0.2385
17522	hsa-miR-658	0.138
17322	hsa-miR-659	0.0865
17507	hsa-miR-662	0.2655
17558	hsa-miR-663	-0.253
17939	hsa-miR-671-5p	-0.0475
3980	hsa-miR-7	1.513
17809	hsa-miR-769-3p	-0.0185
3320	let-7a-e	-0.9495

Table 2. Detailed summary of copy number differences between CPT-K5 and RPMI-8402.

Chromosome Region	Copy Number Change	Length	Cytoband	Probes
chr1:0-20,494,568	CN Loss	20494568	p36.33 - p36.12	24
chr1:32,037,807-119,604,973	CN Loss	87567166	p35.2 - p12	76
chr1:152,029,761-154,307,350	CN Loss	2277589	q21.3 - q22	6
chr1:162,537,416-166,302,136	CN Gain	3764720	q23.3 - q24.2	5
chr1:172,149,901-247,249,719	CN Loss	75099818	q25.1 - q44	62
chr2:18,578,430-20,126,698	CN Loss	1548268	p24.2 - p24.1	3
chr2:97,587,717-123,022,648	CN Gain	25434931	q11.2 - q14.3	22
chr2:127,171,541-127,896,686	CN Loss	725145	q14.3	2
chr2:142,784,317-143,583,340	CN Gain	799023	q22.2	2
chr2:195,311,345-196,645,914	CN Gain	1334569	q32.3	3
chr2:213,254,075-240,645,679	CN Gain	27391604	q34 - q37.3	24
chr3:17,263,318-42,692,402	CN Gain	25429084	p24.3 - p22.1	22
chr3:51,558,900-58,238,204	CN Loss	6679304	p21.2 - p14.3	9
chr3:98,619,554-130,084,769	CN Loss	31465215	q11.2 - q21.3	35
chr3:156,726,065-199,501,827	CN Loss	42775762	q25.31 - q29	36
chr4:28,353,752-48,603,922	CN Gain	20250170	p15.1 - p12	12
chr4:52,443,835-82,265,991	CN Loss	29822156	q12 - q21.21	25
chr4:88,817,462-91,838,793	High Copy Gain	3021331	q22.1	6
chr4:94,750,635-112,410,115	CN Loss	17659480	q22.2 - q25	23
chr4:148,951,472-153,057,309	CN Gain	4105837	q31.23 - q31.3	7
chr4:166,329,737-184,463,845	CN Gain	18134108	q32.3 - q35.1	12
chr4:189,753,020-191,273,063	CN Loss	1520043	q35.2	4
chr5:85,726,182-90,885,353	CN Gain	5159171	q14.3	6
chr5:170,685,783-180,289,116	CN Loss	9603333	q35.1 - q35.1	10
chr6:6,200,184-45,777,755	CN Loss	39577571	p25.1 - p12.3	49
chr6:46,977,212-48,422,707	High Copy Gain	1445495	p12.3	2
chr6:48,422,707-54,815,484	CN Gain	6392777	p12.3 - p12.1	8
chr6:82,596,836-107,066,352	High Copy Gain	24469516	q14.1 - q21	22
chr6:122,639,064-130,318,784	CN Gain	7679720	q22.31 - q22.33	4
chr7:0-110,905,368	CN Gain	110905368	p22.3 - q31.1	117
chr7:140,475,283-150,561,002	CN Loss	10085719	q34 - q36.1	11
chr8:48,765,785-51,574,358	CN Gain	2808573	q11.21 - q11.22	6
chr8:52,848,657-54,021,980	CN Loss	1173323	q11.23	3
chr8:107,896,868-113,575,881	CN Gain	5679013	q23.1	7
chr9:0-46,494,788	CN Loss	46494788	p24.2 - p11.2	49
chr9:79,930,525-83,025,183	CN Gain	3094658	q21.2 - q21.31	5
chr10:5,760,948-30,925,931	CN Loss		p15.1 - p11.23	28
chr10:45,156,792-103,362,073	CN Gain	58205281	q11.21 - q24.32	38
chr10:105,926,689-113,958,431	CN Gain	8031742	q25.1 - q25.2	10
chr10:126,098,889-135,374,737	CN Loss	9275848	q26.13 - q26.3	8
chr11:1,685,355-134,452,384	CN Loss	132767029	p15.5 - q25	135
chr12:10,206,738-11,634,172	CN Gain	1427434	p13.2	3
chr12:87,638,698-91,286,429	CN Gain	3647731	q21.33 - q22	4

chr13:19,829,530-112,820,509	CN Gain	92990979	q12.11 - q34	72
chr14:19,650,680-54,473,616	CN Loss	34822936	q11.2 - q22.3	24
chr14:63,421,398-87,578,118	CN Gain	24156720	q23.2 - q31.3	33
chr14:100,378,502-106,368,585	CN Gain	5990083	q32.2 - q32.33	6
chr15:22,563,293-29,287,342	CN Loss	6724049	q11.2 - q13.3	19
chr16:3,471,709-26,676,469	CN Gain	23204760	p13.3 - p12.1	22
chr16:30,643,893-31,072,620	CN Loss	428727	p11.2	2
chr16:51,568,074-81,200,500	CN Gain	29632426	q12.2 - q23.3	31
chr17:22,200,000-74,700,285	CN Loss	52500285	q11.1 - q25.3	75
chr19:9,429,194-13,816,012	CN Loss	4386818	p13.2 - p13.12	5
chr19:40,331,798-41,911,898	CN Loss	1580100	q13.12	3
chr19:51,084,950-55,055,775	CN Loss	3970825	q13.32 - q13.33	7
chr19:55,055,775-56,409,738	CN Gain	1353963	q13.33	4
chr20:6,280,604-22,537,192	CN Gain	16256588	p12.3 - q11.21	2
chr20:29,580,115-62,435,964	CN Loss	32855849	q11.21 - q113.33	50
chr22:15,885,350-16,042,988	CN Gain	157638	q11.1	4
chr22:25,646,188-30,884,050	CN Gain	5237862	q12.1 - q12.3	10
chrX:0-154,913,754	CN Loss	154913754	p22.32 - q28	169